Fluctuations, ELM Filaments and Turbulent Transport in the SOL at the Outer Midplane of ASDEX Upgrade

H.W. Müller[1], J. Adamek[2], R. Cavazzana[3], G.D. Conway[1], J.P. Gunn[4], A. Herrmann[1], J. Horacek[2], C. Ionita[5], M. Kocan[1], M. Maraschek[1], C. Maszl[5], F. Mehlmann[5], B. Nold[6], M. Peterka[7], V. Rohde[1], R. Schrittwieser[5], N. Vianello[3], E. Wolfrum[1], M. Zuin[3], and the ASDEX Upgrade Team[1]

[1] Max-Planck-Institut für Plasmaphysik, EURATOM Association, 85748 Garching, Germany
[2] Institute of Plasma Physics, Association EURATOM/IPP.CR, Prague, Czech Republic
[3] Consorzio RFX, Associazione EURATOM-ENEA sulla Fusione, Padova, Italy
[4] CEA, IRFM, F-13108 Saint-Paul-lez-Durance, France
[5] Institute for Ion Physics and Applied Physics, University of Innsbruck, Association EURATOM/ÖAW, Austria
[6] Institut für Plasmaforschung, Universität Stuttgart, Stuttgart, Germany
[7] Faculty of Mathematics and Physics, Charles University of Prague, Czech Republic

E-mail contact of main author: hans.werner.mueller@ipp.mpg.de

Abstract. This paper presents turbulence investigations in the SOL at the outboard side of ASDEX Upgrade in ohmic, L-mode and H-mode discharges using electrostatic and electromagnetic probes. Detailed studies are performed on small scale turbulence and on ELM filaments. Simultaneous measurements of floating and plasma potential fluctuations revealed significant differences. They can cause large errors when extracting the electric field from floating potential measurements, even in ohmic discharges. Turbulence studies in ohmic plasmas show the existence of density holes inside the separatrix and blobs outside. Close to the separatrix a reversal of the poloidal blob propagation velocity occurs. Studies on the Reynolds stress in the scrape-off layer show its importance for the momentum transport in L-mode while its role for momentum transport during ELMs in H-mode is rather small. For the first time the electron density and temperature were measured ELM filament resolved in type-I ELMy H-mode. Investigations on the ions in the filaments by a retarding field analyser indicate ion temperatures of 50-80eV in the far SOL. ELMs do not only expel particles and energy into the scrape off layer but also current concentrated in current filaments. Also discharges with type-II ELMs were studied. Comparing the turbulent radial particle transport in discharges with type-I and type-II ELMs at otherwise unchanged global plasma parameters reveal an increased turbulent radial particle flux in the type-II ELMy H-mode.

1. Introduction

Plasma wall interaction is one of the major concerns for future fusion devices [1]. Particle fluxes to the wall cause erosion while heat fluxes have to be limited to exclude a thermal overload of the plasma facing components. In tokamaks a significant fraction of the particle and energy loss is caused by turbulence, either due to small scale turbulence like in ohmic and L-mode discharges and in between ELMs of H-mode discharges or by large transport events (filaments) during ELM activity in H-mode.

Turbulence is a key player in the plasma edge. Turbulence transports particles, energy and momentum in the edge and the scrape-off layer (SOL). But small scale turbulence is also expected to generate large scale flows like zonal flows via the Reynolds stress [2]. The propagation of small turbulent structures is influenced by the ExB velocity (v_{ExB}) which shear is supposed to destroy large structures. This altogether leads to a complex interplay of small and large scale turbulent structures which is also related to the formation of transport barriers [3]. Albeit the large interest for turbulence physics in the edge and scrape-off layer of tokamaks, many questions remained unanswered so far. This paper presents the latest progress in turbulence studies performed in the SOL at the outer midplane of ASDEX Upgrade using

electrostatic and electromagnetic reciprocating probes. The latest results of turbulence investigations with Doppler reflectometry on ASDEX Upgrade are presented in [3].

The paper is organised as follows; in section two the main features of the experimental setup are described. In the third section the experimental findings on small scale turbulence and the related electric fields in ohmic and L-mode discharges are presented. The next section is devoted to new temperature measurements in the SOL of ASDEX Upgrade. In section 5 we report about current filaments associated with ELMs. Turbulent transport properties in discharges with type-II ELMs are presented in section 6. The paper concludes with a summary.

2. Experimental setup

ASDEX Upgrade [4] is a mid size tokamak with a major radius of R = 1.65m and a minor radius of a = 0.5m. If not stated otherwise the discharges presented in this paper were in single null configuration with the ion diamagnetic drift towards the active lower divertor. For the Langmuir probe measurements a fast reciprocating probe (FRP) [5] was operated, which is located 30cm above the equatorial plane. The FRP is equipped with a pneumatic drive allowing for a 100mm stroke in 100ms. It can be equipped with different probe heads. For the investigations presented here several probe heads were operated. For small scale turbulence measurements a multi pin probe head (MP) [6], a probe head which allows for combined electrostatic and electromagnetic measurements (P6M1) [7] and a ball pen probe (BPP) were used [8,9]. A retarding field analyser (RFA) [10] was operated in ELMy H-mode. For investigations were high heat loads can occur a Mach type probe head with ten in-plane Langmuir probes (HHF) [11] similar to flush mounted probes was applied. Five pins were poloidally staggered at each side of the probe. The MP carries 14 proud pins distributed in three radially staggered planes, while the P6M1 has six proud pins of which one is protruding by 3mm compared to the others and a triple coil measuring the time derivative of all three components of the magnetic field. The BPP was exposed to the SOL of a mid size tokamak for the first time. It consists of four proud pins and four retracted ball pen pins which allow for a direct measurement of the plasma potential V_{pl} [8]. Also a new RFA was operated at ASDEX Upgrade. It measures ion temperatures T_i and ion energy distributions. The probe setup is Mach type allowing to sample ions from both directions parallel to the magnetic field B [12]. The data acquisition frequency of all electrostatic and electromagnetic measurements is 2MHz with exception of the RFA collectors which data were sampled at 30kHz.

3. Turbulence and electric field in ohmic and L-mode discharges

In a series of ohmic discharges the basic properties of small scale turbulence were investigated in ohmic ASDEX Upgrade discharges using the multi pin probe in the discharge #24111 [6]. The plasma current was $I_p = 0.8$MA, the toroidal magnetic field $B_t = -2$T, and the line averaged electron density $n_{e,l} = 4.2 \times 10^{19}$m^{-3}. The ion saturation current fluctuations $I_{sat,fl}$ are expected to be dominated by electron density fluctuations $n_{e,fl}$ and therefore $I_{sat,fl}$ is used as a measure of $n_{e,fl}$. In this paper the index $_{fl}$ is always indicating fluctuations of a quantity. The PDFs of the $I_{sat,fl}$ clearly indicated that density blobs and holes are born close to the separatrix. While the blobs are moving outward the holes exist in a few mm wide area inside the separatrix. Blobs carry in the SOL of L-mode discharges an outward radial particle flux as shown in [7]. The propagation velocity of the fluctuations perpendicular to B, shown in figure 1 for an ohmic discharge at $n_{e,l} = 2.6 \times 10^{19}$m^{-3}, is determined by cross correlation of two poloidally separated probe pins both measuring I_{sat} [13]. A velocity shear is visible in the SOL
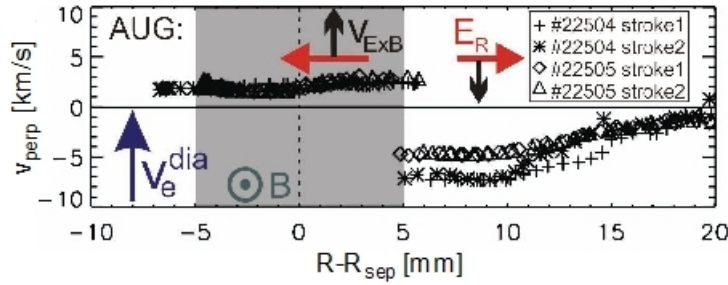
Figure 1: Radial profile of the perpendicular fluctuation propagation velocity. In the plot are also indicated the direction of the magnetic field B, the radial electric field E_r (in red) and the diamagnetic electron drift direction v_e^{dia}. The shaded area represents the uncertainty of the separatrix position.

accompanied by an abrupt flow reversal just outside the separatrix. The measurements do not show a smooth transition but a sudden jump between the two directions of motion which was well reproduced for four strokes. Profiles of the perpendicular velocity from probe cross correlation agree well with the velocity profile measured using the Doppler reflectometry technique [6], where the movement of turbulent density fluctuations is detected using the Doppler radar principle [3]. The frequency of the backscattered signal is Doppler shifted by $\omega = k_\perp u_\perp$, where $u_\perp = v_{ExB} + v_{ph}$ is the fluctuation propagation velocity. The main difference is the smooth transition of the propagation direction seen by the Doppler reflectometry. This might be attributed to the different diagnostic techniques applied.

Doppler reflectometry is able to measure the radial electric field $E_r = - u_\perp B$ when the turbulence phase velocity v_{ph} is small compared to the v_{ExB} – which is generally the case. A common technique to derive E_r from Langmuir probe diagnostics are V_{flt} measurements at radially staggered Langmuir pins. The mean radial electric field $<E_r>$, where $<...>$ denotes a time average is then calculated by $<E_r> = (<V_{flt,1}> - <V_{flt,2}>)/d_r$ with the radial tip distance d_r between pin 1 and 2. Plasma potential V_{pl} and V_{flt} are related via the electron temperature T_e via $V_{flt} = V_{pl} - \alpha T_e$ with $\alpha \approx 2.8$ [14]. This offers a possibility to determine $<E_r>$ by measuring the $<V_{flt}>$ and electron temperature profile $<T_e>$ (taking the data from Thomson scattering) simultaneously and calculating $<E_r> = -grad_r(<V_{flt}> + \alpha <T_e>)$.

Figure 2: Comparison of E_r profile deduced from BPP and Doppler reflectometry.

Both methods were applied for the ohmic discharge #24111 and result in an $<E_r>$ profile which is not in agreement with the Doppler data in the steep gradient region ($R - R_{sep} < 1cm$), while the probe cross correlation fits well to the Doppler measurement. This indicates that the assumption of an homogeneous T_e over d_r is not valid close to the separatrix. Using time averaged data from probes and Thomson scattering also fails to determine V_{pl} correctly. So, most probably $T_{e,fl}$ influences the probe and Thomson measurements differently.

The BPP is predicted to measure V_{pl} directly [8] which was already tested in small devices [15]. Recent experiments have shown that the BPP is also applicable to the SOL of mid size tokamaks [9]. Figure 2 shows the comparison of E_r directly calculated from the V_{pl} of the BPP to data from the Doppler reflectometer. The discharge (#24349) was in L-mode at $I_p = 0.8MA$, $B_t = -2.3T$, and $n_{e,l} = 3.2x10^{19}m^{-3}$, $P_{NBI} = 1MW$. The profile derived from the BPP data agrees well with E_r calculated from the Doppler reflectometer which supports the assumption that the

poloidal motion of the density fluctuations is in fact governed by v_{ExB} and $v_{ph} \ll v_{ExB}$. The comparison also gives confidence that BPPs can be used in the SOL of mid size tokamaks to
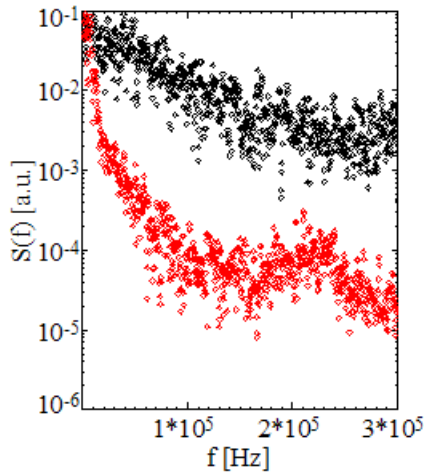

Figure 3: Comparison of the power spectrum of V_{flt} (black) and V_{pl} (red).

measure V_{pl}, at least in L-mode. The fact that $\langle E_r \rangle$ cannot be correctly derived from V_{flt} due to T_e fluctuations as mentioned in the previous paragraph is supported by a comparison of the V_{pl} and V_{flt} power spectrum measured simultaneously by the BPP in the SOL as shown in figure 3. The data are taken in a L-mode discharge (#24348) with $I_p = 0.8$MA, $B_t = -2.3$T, and $n_{e,l} = 3.2 \times 10^{19}$m^{-3}, $P_{NBI} = 1$MW with the probe located 17mm outside the separatrix. It is obvious that the turbulence level in V_{flt} is significantly higher than in V_{pl} especially at frequencies above 10kHz. The same observation was made in H-mode in between ELMs [9]. The difference in the power spectra is attributed to T_e fluctuations. Modelling results are in line with this interpretation. ESEL code runs show that the length scale of $T_{e,fl}$ due to a blob is much smaller than the spatial scale of V_{pl} [16] while the relative fluctuation levels of V_{pl} and αT_e are about the same. Both fluctuations are attributed to the same sequence of events, therefore moving with the same velocity. Consequently $T_{e,fl}$ allows for higher fluctuation frequencies in V_{flt} compared to V_{pl}. An equivalent observation was made for ELM filaments in H-mode. The most reliable method to determine the radial velocity v_r is a cross correlation of radially staggered I_{sat} measurements while calculating v_r from ExB using V_{flt} measurements is strongly affected by the spatial arrangement of the probe pins and the time interval for data averaging [17]. This indicates that turbulent structures and diagnostic are of comparable size. On average v_r deduced from ExB using V_{flt} data is lower than the value from the cross correlation of I_{sat} pins.

A simultaneous measurement of V_{pl} and V_{flt} allows to determine T_e and to compare the mean
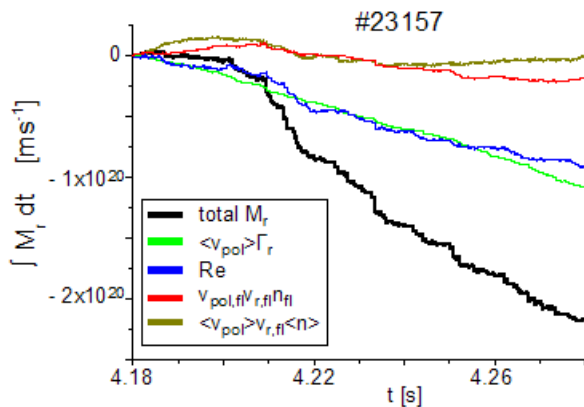

Figure 4: Integrated radial transport of poloidal momentum in a L-mode discharge.

profile with other diagnostics to test if the approximation $V_{flt} = V_{pl} - \alpha T_e$ is valid. In the L-mode discharge #24349 a fair agreement between T_e derived from the potentials and T_e of a swept single probe was found in the SOL for R - R$_{sep}$ > 1cm [9]. At the innermost position the T_e profile connects well to the Thomson scattering T_e profile. Summarising these observations it was found that close to the separatrix V_{pl} cannot be approximated by $V_{flt} + \alpha T_e$ since T_e fluctuations cannot be neglected and seem to affect the measurement. Also in ELM filament studies the approximation is strongly limited since the substructure of the filament is of the same size as the measurement arrangement. For mean profiles in the SOL (R-R$_{sep}$ > 1cm) at least in L-mode the relation $V_{flt} = V_{pl} - \alpha T_e$ seems to hold. Further investigations on this subject will follow.

Investigations of turbulence induced radial transport of poloidal momentum have been performed with the P6M1 probe [18]. The probe was located in the far SOL during L-mode

Figure 5: Time integrated radial transport of poloidal momentum during an H-mode discharge.

and H-mode discharges and the position was kept constant during the measurement. For these investigation it has to be assumed that the electric fields derived from V_{flt} are not strongly affected by T_e fluctuations. In the far SOL of L-mode discharges this should be a reasonable approximation although for quantitative studies the influence of $T_{e,fl}$ has to be investigated. The measurement was performed in a purely ohmic discharge so there was no external momentum input. The plasma parameters are I_p= 0.8MA, B_t = -2.5T, and $n_{e,l}$ = 4.9×10^{19}m^{-3}. The probe location was 45mm outside the separatrix. The radial transport of poloidal momentum $M_r = n v_r v_{pol}$ can be split into the convective part due to the turbulent radial particle flux $\Gamma_r <v_{pol}>$, the Reynolds stress Re = $<n> v_{r,fl} v_{pol,fl}$, and a pure fluctuation contribution $n_{fl} v_{r,fl} v_{pol,fl}$. Figure 4 shows the integrated radial transport of poloidal momentum. It is obvious that the momentum transport is dominated by the convective part due to the turbulent radial particle transport $\Gamma_r <v_{pol}>$ and the Reynold stress Re. The transport is outward for a momentum in direction of the ion diamagnetic direction which is towards the active divertor and counter current direction. This direction of the poloidal momentum agrees with the poloidal propagation velocity in the SOL shown in figure 1. The situation changes in H-mode as shown in figure 5. The parameters of #23163 were I_p= 0.8MA, B_t = -2.5T, and $n_{e,l}$ = 6.2×10^{19}m^{-3}, heating power of the neutral beam injection P_{NBI} = 2.5MW. The probe was 38mm outside the separatrix. In H-mode the Reynolds stress term is small compared to the convective and the triple fluctuation term $n_{fl} v_{r,fl} v_{pol,fl}$. Also visible, the mean transport is in the opposite direction dominated by the ELM bursts while in between ELMs the radial transport of poloidal momentum is in the same direction as in L-mode. Although the data values in H-mode might be affected by rather large errors in the calculation of the electric fields, especially during ELMs, the general trend is expected to hold.
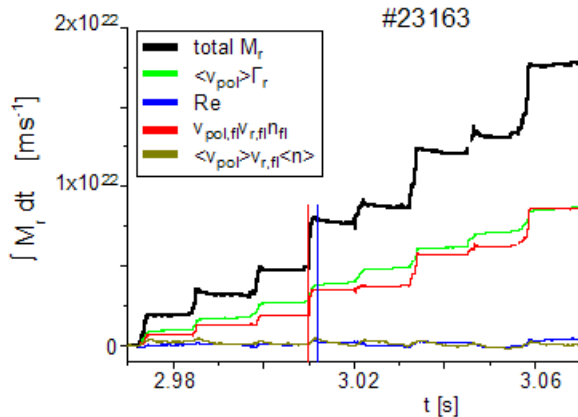
4. ELM filament temperatures

ELMs having a filamentary structure can transport significant energy to the first wall which is a potential hazard for next step fusion devices. Therefore, it is of great interest to gain knowledge on the electron T_e and ion T_i temperature development in filaments travelling across the SOL. For the first time experiments were performed to measure T_e of individual ELM filaments with 5-10μs time resolution using single probes with fast swept bias voltage (HHF probe head). In L-mode discharges the comparison of slow (kHz range) and fast swept single probes indicated that at bias sweep frequencies of 50-100kHz the probe characteristics still can be used to determine n_e and T_e [11]. In a type-I ELMy H-mode plasma (#24925) with I_p = 0.8MA, B_t = -2.5T, P_{NBI} = 3.6MW, electron cyclotron heating power P_{ECRH} = 1.5MW, and $n_{e,l}$ = 6.1×10^{19}m^{-3} ELM filaments are detected with 10μs time resolution 4.5cm outside the separatrix. Figure 6 shows n_e, T_e, V_{flt}, and beta determined from the fast swept single probe (black data) during an ELM starting at t = 3.980s. Beta is the ratio of electron to ion saturation current being calculated in the fitting procedure of the characteristic. Data with beta above 30

are removed since they are usually related to a bad fit of the characteristic. The stars (diamonds) indicate results while sweeping the bias voltage from positive (negative) to negative (positive). For comparison the V_{flt} data of a nearby floating Langmuir pin is shown in red (data are taken at 2MHz). A very good agreement is observed. The differences can mainly be attributed to the different time resolution. During the ELM n_e and T_e peaks of $n_e = 1\text{-}2*10^{19}m^{-3}$ and $T_e = 30\text{-}40eV$ are detected in ELM filaments. From 3.9805s on there is a good correlation of $n_{e,fl}$ and $T_{e,fl}$ (see also [11]). It is not yet clear why there are no correlated fluctuations in the beginning of the ELM. In [11] a comparison is presented on a smoothed ELM T_e (25µs time resolution) derived from the BPP and a fast swept single probe (100kHz bias sweep). Both methods agreed well and delivered $T_e = 10\text{-}15eV$ during type-I ELM activity at the position of the outer limiter 5.5cm outside the separatrix.
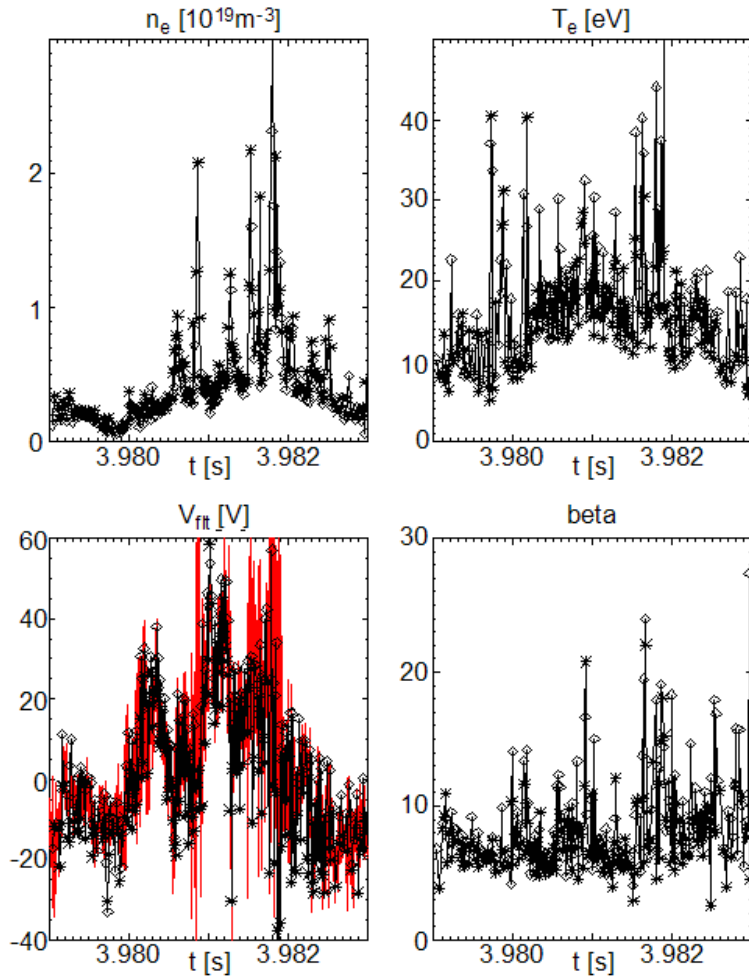

Figure 6: Electron density, temperature and floating potential fluctuations during an ELM. The ratio of ion and electron saturation current (beta) is also shown.

Investigations on T_i in ELM filaments indicate that $T_i > T_e$. In [19] T_i was derived from the power load and I_{sat} fall off lengths in the SOL during ELM activity delivering $T_i = 30 - 60eV$. This is supported by the first RFA data from ASDEX Upgrade showing $T_i = 50 - 80eV$ in the far SOL when filaments pass by [10]. This ELM filament T_i is consistent to the current ELM transport models [20,22]. There is strong evidence that the ion impact energies exceed 160eV in the far SOL during ELMs [10] which fits to the observed T_i. The ion energy data are consistent with measurements from JET [21], raising concerns on the first wall life time in future fusion devices when unmitigated ELMs are present.

5. Current Filaments

Experiments indicated that ELMs do not only release particles and energy from the confined plasma but also, as expected, current. In previous experiments at ASDEX Upgrade pick up coils were used to detect currents related to the ELM events [23]. The magnetic fluctuations detected during ELMs have been explained by mode structures in the confined plasma carrying a bidirectional current. In recent experiments the P10M1 probe head allowed for a simultaneous measurement of the fluctuations in all three components of B with enhanced spatial resolution [24,25]. Also the applied analysis methods were more advanced. Figure 7

shows the degree of polarisation (DOP) during a type-I ELMy H-mode (#23159). The plasma parameter are $I_p = 0.8MA$, $B_t = -2.5T$, $P_{NBI} = 2.5MW$, and $n_{e,l} = 6.1\times10^{19}m^{-3}$. The probe head was 12mm in front of the limiter. The DOP is a test of the plane wave ansatz for the measured magnetic signature [25]. The reduction of the DOP with each ELM event (indicated by I_{sat}) shows that the magnetic signature of the magn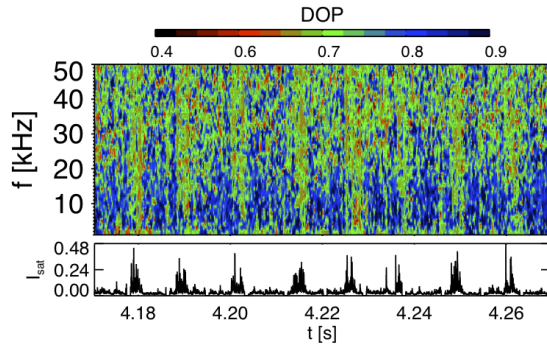etic fluctuations B_{fl} is no longer compatible to a plane wave and therefore most probably associated to a localised structures. The analysis of the magnetic signals reveals that the direction of minimum B_{fl} is well aligned to the local B. Within the ELM activity the B_{fl} components in the plane perpendicular to B show a phase relation compatible to current filaments extended parallel to B carrying a mono polar current. These current filaments are located outside the separatrix at the outer midplane and show current densities up to $6MAm^{-2}$. Possibly the filaments are still connected to the confined plasma allowing for such high current densities although heat load measurements during ELM activity indicted that ELM filaments hitting the outboard limiters in ASDEX Upgrade are detached from the confined plasma [19]. A simultaneous I_{sat} measurement cannot be used to verify the ELM filament´s current density since the probe tip introduces a sheath resistance inhibiting high current densities.

Figure 7: Top: DOP analysis of magnetic signature. Bottom: I_{sat} signal indicating ELM activity.

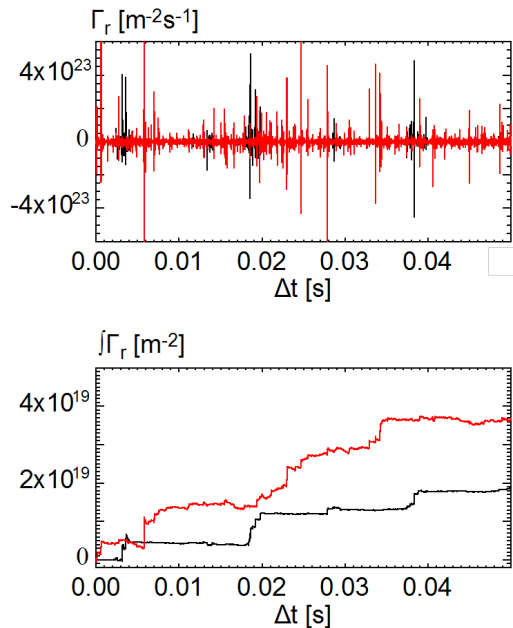## 6. Turbulent transport in type-II ELMy H-mode

Figure 8: Top: time trace of the turbulence induced radial particle flux for a type-I ELMy (black) and type-II ELMy (red) H-mode). Bottom: time integral of the radial flux.

In a series of discharges a transition from type-I ELMy H-mode to type-II ELMy H-mode was induced by varying the closeness to double null. The global plasma parameters like energy content etc. stayed about constant. The presented data originate from discharge #25727 with the following plasma parameters: $I_p = 0.8MA$, $B_t = -2.5T$, $P_{NBI} = 7.5MW$, $P_{ECRH} = 0.8MW$, and $n_{e,l} = 5.5\times10^{19}m^{-3}$. The turbulence induced radial flux in both phases of the discharge is shown in figure 8 while the probe was at a distance of about 6.5cm to the separatrix. In the type-I period (black) well separated bursts indicate the ELMs. In the type-II ELM period (red) the transport bursts are much more equally distributed in time. The time integrated flux clearly shows that the average particle flux is significantly higher during the type-II ELMy H-mode (red). The positive sign corresponds to an outward particle flux. In the type-II ELMy phase still rather large transport events can occur on the outer midplane visible at steps in the particle transport. Since the poloidal electric field E_{pol} again had to be determined from V_{flt} there might be a rather large error in the amplitude but the general trends are expected to be robust.

7. Summary

The origin of blobs and holes in ohmic discharges was identified to be close to the separatrix. T_e fluctuations cannot be neglected in ohmic and L-mode discharges at ASDEX Upgrade when investigating turbulence, especially close to the separatrix. Neglecting $T_{e,fl}$ might lead to errors when V_{pl} is calculated from V_{flt} even when using time averaged values. Electric fields during ELM activity in H-mode derived from V_{flt} can also be affected by $T_{e,fl}$ causing rather large uncertainties. The poloidal momentum transport in the SOL was measured for the first time in ASDEX Upgrade showing the importance of the Reynolds stress in L-mode. ELM filament resolved T_e measurements indicated rather hot ELM filaments (several 10eV) in the far SOL while T_i is in the range 50-80eV. ELMs are associated with field aligned current filaments carrying currents up to ~ kA. In type-II ELMy H-modes the outward radial particle flux is enhanced compared to type-I ELMy H-mode at about the same global plasma parameters.

References
[1] A. Loarte et al., Proc. 22nd IAEA FEC, Geneva, IAEA-CN-165/IT/P6-13
[2] B. Scott, Phys. Lett. A **320** (2003) 53
[3] G.D. Conway, IAEA-CN-180/EXC/7-1, this conference
[4] A. Herrmann, O. Gruber, Fusion Science and Technology **44** (2003) 569
[5] V. Rohde et al., ECA 20C (EPS 1996), Kiev, D040
[6] B. Nold et al., Plasma Phys. Control. Fusion **52** (2010) 065005
[7] C. Ionita et al., J. Plasma Fusion Res. **8** (2009) 413
[8] J. Adamek et al., J. Nucl. Mat. **390-391** (2009) 1114
[9] J. Adamek et al., Contr. Plasma Phys. **50** (2010) 853
[10] M. Kocan et al., Plasma Phys. Control. Fusion, submitted
[11] H.W. Müller et al., Contr. Plasma Phys. **50** (2010) 847
[12] M. Kocan et al., Contr. Plasma Phys. **50** (2010) 836
[13] U. Stroth et al., Proc. 22nd IAEA FEC, Geneva, IAEA-CN-165/EX/P4-23
[14] V. Rohde and ASDEX Upgrade Team, Contr. Plasma Phys. **36** (1998) 109
[15] J. Adamek et al., Czech. J. Phys. **55** (2005) 235
[16] J. Horacek et al., Nucl. Fusion, **50** (2010) 105001
[17] A. Kirk et al., Plasma Phys. Control. Fusion, submitted
[18] F. Mehlmann et al., EPS Conference on Plasma Physics 2010, Dublin, P1.1064
[19] A. Herrmann et al., J. Nucl. Mater **363-365** (2007) 528
[20] W. Fundamenski, Plasma Phys. Control. Fusion **48** (2006) 106
[21] R.A. Pitts et al., Nucl. Fusion **46** (2006) 82
[22] A. Kirk et al., J. Nucl. Mater. **390-391** (2009) 727
[23] A. Herrmann et al., Proc. 22nd IAEA FEC, Geneva, IAEA-CN-165/EX/P6-1
[24] E. Martines et al., Plasma Phys. Control. Fusion **51** (2009) 124035
[25] N. Vianello et al., Phys. Rev. Lett., submitted